

# Thickness dependence of Shockley-type surface states of Ag(111) ultrathin films on Si(111) $7\times 7$ substrates

Keiichi Sawa, Yuki Aoki, and Hiroyuki Hirayama\*

*Department of Materials Science and Engineering, Tokyo Institute of Technology, J1-3, 4259 Nagatsuda, Midori-ku, Yokohama 226-8502, Japan*

(Received 5 June 2009; revised manuscript received 7 July 2009; published 28 July 2009)

We studied the surface-state dispersion of ultrathin Ag(111) epitaxial films on Si(111) substrates by analyzing the bias-voltage dependence of surface electron standing-wave patterns using a scanning tunneling microscope. The 40-monolayer (ML)-thick Ag film exhibited a two-dimensional, free-electronlike surface-state dispersion similar to that of the bulk Ag(111) surface. However, the bottom of the surface-state band ( $E_0$ ) shifted from  $-51$  to  $+26$  meV with respect to the Fermi level as the Ag film thickness decreased from 40 to 7 ML. The effective mass of the surface electron decreased slightly as film thickness decreased. The shift in  $E_0$  is reasonably attributed to the modification of the electronic structure induced by thickness-dependent misfit-strain relaxation. In contrast to the Ag/Ge(111) system, the surface state hybridizes with neither the substrate bulk band nor the Ag film's quantum-well state in the Ag/Si(111) system.

DOI: [10.1103/PhysRevB.80.035428](https://doi.org/10.1103/PhysRevB.80.035428)

PACS number(s): 73.20.At, 73.40.Ns

## I. INTRODUCTION

The (111) surface of Ag bulk crystal has a Shockley surface state, which reveals free-electronlike parabolic dispersion.<sup>1,2</sup> The bottom of the surface band is located 63 meV below the Fermi level and its effective mass is  $0.42m_0$  ( $m_0$  is the static mass of the electron).<sup>3</sup> In principle, (111)-oriented Ag films are expected to have the same surface state as bulk Ag(111) surfaces. However, surface-state dispersion has been reported to be modified for ultrathin Ag(111) epitaxial films grown on metal and semiconductor substrates.<sup>4–11</sup>

On Au(111) substrates, ultrathin Ag(111) films initially have a surface state close to the intrinsic surface state of Au(111) substrates ( $-475$  meV with respect to the Fermi level). However, the surface state gradually shifts upward toward the intrinsic surface state of Ag(111) as film thickness increases.<sup>4,5</sup> A similar thickness-dependent shift in the surface state was reported in the epitaxial growth of Ag (111) films on a single monolayer (ML) Au film deposited on Ag(111) substrates.<sup>6</sup> Two surface states, the Shockley intrinsic surface state of the substrate and the Ag-induced surface state, were observed for ultrathin Ag(111) films grown on Cu(111) substrates.<sup>7</sup> In every case, the Ag(111) films revealed a surface state close to the metal substrates in the initial stage of the growth. The surface states approached to the intrinsic state of the bulk Ag(111) surface with an increase in Ag film thickness.

In contrast to Ag films on metal substrates, no Shockley surface state exists in the initial growth of Ag films on semiconductor substrates. The Shockley surface state starts to evolve only after the growth of the Ag film of a certain thickness. For Ag(111) epitaxial films on Si(001) substrates, the surface state appears at  $\sim 4$  ML.<sup>8</sup> Furthermore, on the semiconductor substrates, the surface dispersion of the ultrathin Ag(111) films is different from that of the bulk Ag(111) surface. An unusual, nonparabolic dispersion was reported for the surface state of ultrathin Ag(111) films grown on Ge(111) substrates.<sup>9,10</sup> This anomaly in the dispersion was

attributed to the hybridization of the intrinsic Ag surface state with the substrate bulk band. For ultrathin Ag(111) films on Si(111) substrates, the surface state disappeared in photoelectron spectroscopy (PES).<sup>11</sup> In this system, ultrathin Ag films have a huge misfit strain due to the 25% difference in the lattice constant between Ag and Si. The disappearance of the surface state in PES suggests that the misfit strain may cause the upward shift of the surface-state energy beyond the Fermi energy, where PES has no access.

In previous studies, PES was adapted to investigate the surface state of ultrathin Ag films.<sup>5–11</sup> However, PES accesses only the states below the Fermi level and does not provide any information on states above the Fermi level. In the meantime, the bottom of the intrinsic parabolic dispersion of the bulk Ag(111) surface states is shallow and very close to the Fermi level. The effective energy region accessed by PES is limited to only a small part of the entire surface band dispersion in  $k_{\parallel}$ . In this respect, it is highly desirable to obtain complementary information on surface-state dispersion above the Fermi level for ultrathin Ag(111) films. In particular, this is the case for Ag on the Si(111) system, in which the upward shift of the surface state has been suggested in PES. In this paper, we report on surface band dispersion in the empty state of ultrathin Ag(111) films epitaxially grown on the Si(111) substrates using a scanning tunneling microscope (STM).

## II. EXPERIMENT

This study was carried out with an ultrahigh-vacuum (UHV) apparatus equipped with a cryogenic sample cooling system, an Ag Knudsen cell, a reflection high-energy electron diffraction, and a low-temperature STM unit. Si(111) substrates were cut from an  $n$ -type wafer, set on the STM sample holder, and preheated at 900 K overnight in the UHV apparatus. They were cleaned by flashing at 1400 K for 10 s and subsequent slow cooling to room temperature. Cleanliness of the substrates was confirmed by observing the defect-free,  $7\times 7$  reconstruction of the Si(111) surface. On the clean

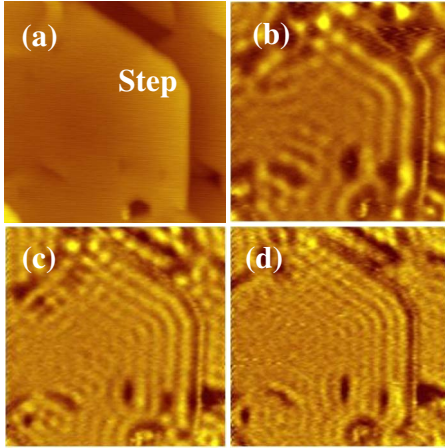


FIG. 1. (Color online) STM image (a) and  $dI/dV$  images (b)–(d) of a 20 ML Ag(111) film surface at liquid  $N_2$  temperature with a tunneling current of 0.55 nA. Sample bias voltage  $V_s$ : (a) 0.35, (b) 0.15, (c) 0.25, and (d) 0.35 V. Image size is 31.5 nm  $\times$  31.5 nm.

substrate, Ag films were deposited at 100 K. The sample was then slowly annealed to 300 K overnight. This two-step process enabled us to obtain Ag(111) epitaxial films of flat morphology.<sup>12</sup> We prepared Ag films with thicknesses  $\theta_{Ag}$  of 7–40 ML.

These Ag films were subjected to STM observation. STM tips were electrochemically etched from polycrystalline tungsten wires. In the UHV apparatus, the tips were cleaned by electron bombardment. During the STM observation, the sample temperature was lowered to  $\sim 70$  K by a supercooled liquid  $N_2$  cryostat attached to the STM unit. We took STM and  $dI/dV$  images simultaneously by applying a small ac modulation voltage ( $V_{p-p}=20$  mV, 1.414 kHz) to the sample bias voltage  $V_s$ .  $dI/dV$  images were obtained using the conventional lock-in technique. The bias voltage  $V_s$  was varied from 0.1 to 0.5 V. The STM image scale at low temperature was calibrated with respect to the  $7 \times 7$  unit cell of the Si(111) clean surfaces.

### III. RESULTS

An observed STM image and the corresponding  $dI/dV$  images of the surface on a 20-ML-thick Ag(111) film on the Si(111) substrate are depicted in Fig. 1 [(a) STM image; (b)–(d)  $dI/dV$  images]. The STM image indicates that most of the Ag film surface is covered by atomically flat terraces, though it includes monolayer steps [as indicated in Fig. 1(a)] and monolayer pits (e.g., the lower right side in the STM image). In addition, partial dislocations (e.g., the lower left side in the STM image) appeared locally at the atomically flat terraces.<sup>12</sup> The  $dI/dV$  images represent the surface electron standing waves that originated from the step edges, the monolayer pit, and partial dislocations.

We deduced the wavelength  $\lambda$  of the surface-state electron from the distance between peaks in the cross-sectional view of the surface electron standing waves. To prevent the cross interaction of standing waves from different origins, we adapted the standing wave extending from the step edge to-

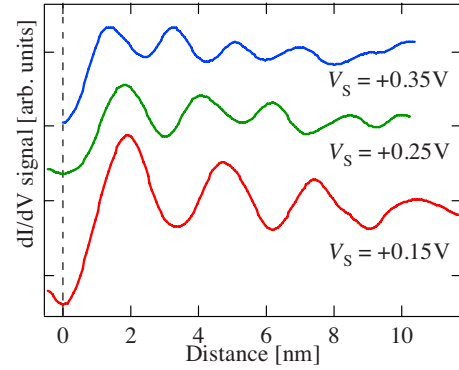


FIG. 2. (Color online) Cross sections of the surface electron standing waves from the step edge to the defect-free area [see Fig. 1(a) and the  $dI/dV$  images of Figs. 1(b)–1(d)]. The step edge (indicated by the dotted line) is considered as the origin of the distance ( $=0$  nm).

ward the defect-free terrace area (e.g., the central part in the figure) for the analysis. The data in the narrow areas surrounded by defects were discarded because the quantum confinements in the narrow regions between steps<sup>13,14</sup> or step dislocation could modify the dispersion relation. Figure 2 presents the cross sections of the electron standing waves of a defect-free area in the  $dI/dV$  images [Figs. 1(b)–1(d)] for several  $V_s$ s. Standing waves oscillate periodically and decay, as they are apart from the step edge at any bias voltage. The distance between peaks corresponds to half of the wavelength of the surface electron  $\lambda/2$ .<sup>15</sup> Using this relation, we deduced  $\lambda$  of the surface electron standing waves in a range of  $V_s=0.1$ – $0.5$  eV for Ag films of various thicknesses.

The dispersion relation of the surface-state electron  $E(k)$  is obtained by plotting the wave vector  $k_{\parallel}=2\pi/\lambda$  parallel to the surface as a function of electron energy  $E$  ( $=$  the bias voltage  $V_s$ ). Results are presented as  $E$  vs  $k_{\parallel}^2$  plots in Fig. 3 for 7-, 10-, 20-, 30-, and 40-ML-thick Ag(111) films. For each thickness, the plot was nicely fitted by a linear line.

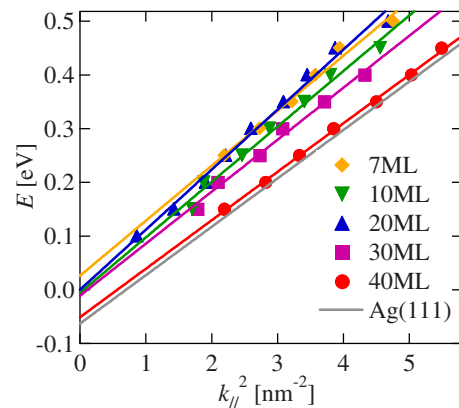


FIG. 3. (Color online) Surface-state dispersion ( $E-k_{\parallel}^2$  relation) of 7 ML (filled diamonds), 10 ML (filled downward triangles), 20 ML (filled upward triangles), 30 ML (filled squares), and 40 ML (filled circles) thick Ag(111) films on the Si(111) substrates. Solid lines denote the parabolic fittings of the experimental data. The surface-state dispersion of the intrinsic surface states of the bulk Ag(111) surface (Ref. 3) is also indicated by the solid line.

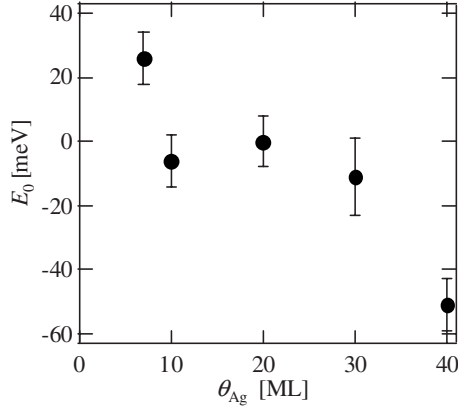


FIG. 4. Film thickness dependence of the band bottom  $E_0$  obtained by the fitting lines in Fig. 3. Experiment errors are  $\pm 8$  meV for 7-, 10-, 20-, and 40-ML-thick films and  $\pm 12$  meV for 30-ML-thick film.

results are evidence that the surface-state preserved parabolic dispersion even for ultrathin Ag(111) films on the Si(111) substrates. Specifically, the 40-ML-thick Ag film exhibited almost the same dispersion as that in the bulk Ag(111) surface with  $E_0 = -63$  meV and  $m^* = 0.42 m_0$ .<sup>3</sup> However, we found that the energy of the intersection at  $k_{\parallel} = 0$  in the fitting line tends to increase as thickness decreases from 40 to 7 ML. The gradient also becomes steeper with a decrease in thickness. We evaluated the bottom of the surface-state band  $E_0$  and the effective mass  $m^*$  from the intersection and gradient of the fitted lines. Within the errors, Fig. 3 provides clear experimental evidence that the surface-state band preserves parabolic dispersion, but  $E_0$  shifts upward over the Fermi level with a decrease in Ag thickness, as suggested in the PES study.<sup>11</sup> Substantially,  $E_0$  shifted from  $-51$  to  $+26$  meV as thickness decreased from 40 to 7 ML, as depicted in Fig. 4 and in the fourth column of Table I. The  $m^*$  changed from  $0.42 m_0$  to  $0.37 m_0$  with a decrease in Ag film thickness, as indicated in the fifth column in Table I. (The error bar in  $m^*$  was  $\pm 0.2 m_0$ .)

#### IV. DISCUSSION

In previous studies, hybridization of the surface state with the substrate band and the QWSs in Ag films were consid-

ered the cause of modified surface-state band dispersion for ultrathin Ag(111) films grown on Ge(111) substrates<sup>9,10</sup> and for ultrathin Ag(111) films covered with 1 ML Bi on Si(111) substrates.<sup>17</sup> In addition, the misfit-strain-induced change in the electron structure of Ag films was suggested as the cause of modification of the surface state of ultrathin Ag(111) films grown on the Si(111) substrates.<sup>11</sup>

First, we discuss whether hybridization with the substrate band could cause the observed thickness-dependent shift in  $E_0$  for our Ag/Si(111) system. As for the decay length of the surface state of Ag(111), which was reported as 2.8 nm ( $\sim 10$  ML),<sup>6</sup> the surface state would increase the overlap with the bulk band as the Ag film thickness decreased, especially below  $\sim 10$  ML. However, the surface state could not hybridize with the substrate bulk band in the Ag/Si(111) system, as in the Ag/Ge(111)<sup>9,10</sup> and Al/Si(111)<sup>18</sup> systems. For Ge, the valence-band maximum (VBM) is very close to the Fermi level at  $\bar{\Gamma}$ . Therefore, even the intrinsic Ag surface state with its bottom at only 63 meV below the Fermi level can intersect the Ge bulk band in the Ag/Ge(111) system. As a result, the surface state hybridizes with the valence band of the substrate Ge. The parabolic dispersion is modified and  $E_0$  is lifted. However, the VBM of Si is located at  $-0.3$  eV.<sup>19</sup> Thus, it can intersect a surface state on the Al films that are further below the Fermi level.<sup>18</sup> It does not, however, intersect with the Ag surface state with its bottom at  $-63$  meV at any  $k$  in the surface plane and cannot hybridize with this surface state.

In contrast to the bulk band, the QWS can intersect the surface-state dispersion in the Ag/Si(111) system. The valence electrons are confined in the narrow space between the surface and the interface to generate one-dimensional QWSs along the surface normal [i.e.,  $\Gamma-L$  (111)] direction in ultrathin Ag(111) films. Because of the specific band dispersion of Ag in the  $\Gamma-L$  direction, QWSs appear only below the Fermi level and shift upward toward the Fermi level as the Ag film thickness increases in the energy region of interest in this study.<sup>16,19-21</sup> Here, the uppermost QWS [ $n=1$  QWS (Ref. 21)] could intersect the intrinsic surface state of the Ag(111) surface.

We calculated the hybridization of the surface state and the  $n=1$  QWS for 7-, 10-, 20-, 30-, and 40-ML-thick Ag(111) films. As an example, the 20-ML-thick Ag film is

TABLE I. Thickness dependence of  $E_0$  and  $m^*$ . First column: Ag film thickness. Second column: bottom of the  $n=1$  QWS estimated in the two-band model calculation (Ref. 16). Third column: crossing point ( $k_{\parallel}$ ) of the intrinsic Ag(111) surface state and the  $n=1$  QWS in-plane dispersions. Fourth and fifth columns: experimentally determined  $E_0$  and  $m^*$ . Sixth and seventh columns: theoretically calculated  $E_0$  and  $m^*$  for  $H_{SQ} = 100$  meV. Eighth and ninth columns: theoretically calculated  $E_0$  and  $m^*$  for  $H_{SQ} = 200$  meV.

| $\theta_{\text{Ag}}$ (ML) | $E_0$ (eV)    |                               | Experiment  |           | $H_{SQ}=100$ (meV) |           | $H_{SQ}=200$ (meV) |           |
|---------------------------|---------------|-------------------------------|-------------|-----------|--------------------|-----------|--------------------|-----------|
|                           | QWS ( $n=1$ ) | Crossing ( $\text{nm}^{-1}$ ) | $E_0$ (meV) | $m^*/m_0$ | $E_0$ (meV)        | $m^*/m_0$ | $E_0$ (meV)        | $m^*/m_0$ |
| 7                         | -1.08         | 4.07                          | 26          | 0.37      | -54                | 0.42      | -27                | 0.41      |
| 10                        | -0.83         | 3.54                          | -6          | 0.37      | -52                | 0.41      | -18                | 0.40      |
| 20                        | -0.45         | 2.51                          | 0           | 0.34      | -52                | 0.38      | -19                | 0.36      |
| 30                        | -0.38         | 2.26                          | -11         | 0.39      | -53                | 0.37      | 28                 | 0.35      |
| 40                        | -0.31         | 2.01                          | -51         | 0.42      | -49                | 0.34      | 46                 | 0.34      |



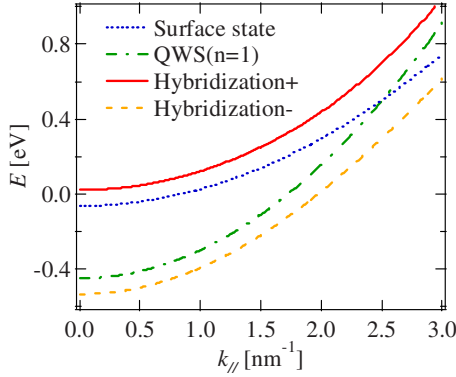


FIG. 5. (Color online) Modification of surface-state dispersion due to hybridization with  $n=1$  QWS. Dotted line: intrinsic Ag(111) surface-state dispersion. Dashed and dotted line: in-plane dispersion of  $n=1$  QWS in the 20-ML-thick Ag film. These dispersions could be modified by hybridization. Solid line: surface-state dispersion modified by hybridization. Dashed line: modified in-plane dispersion of the QWS. In the calculation,  $H_{SQ}$  was taken as 200 meV.

depicted in Fig. 5. In the figure, the in-plane dispersions of the  $n=1$  QWS is denoted by the dashed line and dotted line and the intrinsic surface state of the bulk Ag(111) surface is indicated by the dotted line. Here, we calculated the bottom of the  $n=1$  QWS subband in the two-band model<sup>16</sup> and drew its in-plane dispersion using its effective mass as experimentally reported in the previous PES study.<sup>19</sup> These two states cross at  $k_{\parallel}=2.51 \text{ nm}^{-1}$ . However, the degeneracy at the intersection is lifted off, and the two states split into upper and lower branches by introducing the hybridization interaction  $H_{SQ}=\langle \text{QWS} | V | \text{SS} \rangle$  between the surface state and  $n=1$  QWS at their intersection,<sup>17</sup> indicated by the solid and dashed lines in the figure. The exact value of  $H_{SQ}$  is unknown in the present system. However,  $H_{SQ}$  was reported to range from 20 to 180 meV in Bi/Ag films on the Si(111) substrate system.<sup>17</sup> Thus, we calculated the dispersions of the split branches for  $H_{SQ}=100$  and 200 meV in this study.

We fitted the in-plane dispersion of the upper branch, which stems from the Ag surface state, by a parabolic dispersion curve. Doing so enabled us to extract  $E_0$  and  $m^*$  of the hybridized surface state that are comparable to the experimentally obtained ones. The calculated and experimentally obtained results are listed in Table I. The intersection at which the original dispersion has the largest modification is in the range of  $k_{\parallel}=2-4 \text{ nm}^{-1}$ , as listed in the third column in the table. This range in  $k_{\parallel}$  was fully covered in our standing-wave observations (see the horizontal axis in Fig. 3). Thus, the modification in the surface-state dispersion is expected to manifest itself in the  $E(k_{\parallel})$  plot in Fig. 3 if the hybridization occurs. However, the numerically calculated results suggest thickness dependence in  $E_0$  and  $m^*$ , that is, the opposite of the experiment results. Assuming hybridization, the calculation suggests that  $E_0$  shifts downward and  $m^*$  becomes heavier as the thickness decreases. However, the opposite thickness dependences were observed in the experiment (the fourth and fifth column in Table I). Therefore, we exclude surface-state-QWS hybridization as the cause of the observed shift in the surface states of the Ag(111) films. This calculation indicates that  $H_{SQ}$  is very small and no substan-

tial split occurs in the present Ag/Si(111) system.

Finally, we consider the misfit-strain-induced change in the electronic structure of Ag films as the cause of the shift in  $E_0$ .<sup>11</sup> The lattice constant of Ag is 25% smaller than that of Si. Thus, epitaxially grown Ag films are basically under tensile strain on Si(111) substrates. The strain shifts a conduction-band minimum (CBM) at the gap of the electronic structure of Ag in the  $L$  point. The Shockley surface state of the Ag(111) surface is based on the *real line* connecting the CBM and VBM in the gap at the  $L$  point.<sup>22</sup> Thus, the strain induced change in the bulk electronic structure could cause a shift in the surface state. Empirical pseudopotential method (EPM) calculation demonstrated that the in-plane tensile strain shifts  $E_0$  upward at the Ag(111) film surface.<sup>11</sup>

This misfit-strain-induced change in the electronic structure qualitatively explains our experimental results because the misfit strain is gradually relaxed with film thickness in the heteroepitaxial system.<sup>23</sup> From this viewpoint, it is reasonable to assume that  $E_0$  shifts upward as Ag film thickness decreases since a decrease in thickness increases the in-plane tensile strain. This interpretation is also consistent with the results in a previous PES study of the temperature-dependent shift in  $E_0$  at bulk Ag(111) surfaces.<sup>24</sup> In the PES study, an upward shift in  $E_0$  was observed as the temperature rose. This result also supports the strain-induced upward shift in  $E_0$  for thinner films since a temperature rise causes an expansion of the lattice.

Quantitatively,  $E_0$  shifted upward by 77 meV with a decrease in thickness from 40 to 7 ML in this experiment. Furthermore, the EPM calculation indicated that the 0.95% in-plane tensile strain causes a 150 meV upward shift in  $E_0$ .<sup>11</sup> This result suggests that the accumulated strain in the film was not as great as 25% even in the 7-ML-thick Ag film on the Si(111) substrate. Our previous STM study revealed that Ag films included many partial dislocations even in the very initial growth stage.<sup>12</sup> Tentatively, we attribute the small shift in  $E_0$  to strain relaxation by partial dislocations in Ag films.

## V. SUMMARY

In summary, we studied the thickness dependence of the Shockley surface state of the Ag(111) film surface on the Si(111) substrate. Surface dispersions in the empty state were obtained by measuring the wavelength of the surface electron standing waves at sample bias voltages of +0.1 to 0.5 V in STM-based  $dI/dV$  images. The surface dispersion was parabolic in the Ag/Si(111) system. For the 40-ML-thick Ag film, the bottom  $E_0$  and effective mass  $m^*$  of the surface state were close to those of the bulk Ag(111) surface. However,  $E_0$  shifted upward and  $m^*$  became lighter as thickness decreased. The surface band dispersion did not exhibit the hybridization-induced anomaly reported in the Ag/Ge(111) system because the VBM of Si is located deeper than  $E_0$  of the Ag(111) surface-state band. We also investigated the hybridization of the surface states with the  $n=1$  QWS in Ag films. The numerically expected shift in  $E_0$  and the change in

$m^*$  were the opposite of what we observed. This result indicates that hybridization with the QWS is negligible as the cause of the observed thickness-dependent change in

surface-state dispersion for Ag films. Only a change in the Ag electronic state induced by the misfit strain can reasonably explain the observed thickness dependence.

---

\*hirayama.h.aa@m.titech.ac.jp

- <sup>1</sup>Ph. Avouris, I.-W. Lyo, R. E. Walkup, and Y. Hasegawa, *J. Vac. Sci. Technol. B* **12**, 1447 (1994).
- <sup>2</sup>S. D. Kevan and R. H. Gaylord, *Phys. Rev. B* **36**, 5809 (1987).
- <sup>3</sup>M. Becker, S. Crampin, and R. Berndt, *Phys. Rev. B* **73**, 081402(R) (2006).
- <sup>4</sup>C. Didiot, A. Vedenev, Y. Fagot-Revurat, B. Kierren, and D. Malterre, *Phys. Rev. B* **72**, 233408 (2005).
- <sup>5</sup>H. Cercellier, Y. Fagot-Revurat, B. Kierren, F. Reinert, D. Popović, and D. Malterre, *Phys. Rev. B* **70**, 193412 (2004).
- <sup>6</sup>T. C. Hsieh, T. Miller, and T.-C. Chiang, *Phys. Rev. Lett.* **55**, 2483 (1985).
- <sup>7</sup>A. Bendounan, H. Cercellier, Y. Fagot-Revurat, B. Kierren, V. Y. Yurov, and D. Malterre, *Phys. Rev. B* **67**, 165412 (2003).
- <sup>8</sup>I. Matsuda, H. W. Yeom, T. Tanikawa, K. Tono, T. Nagao, S. Hasegawa, and T. Ohta, *Phys. Rev. B* **63**, 125325 (2001).
- <sup>9</sup>S.-J. Tang, T. Miller, and T.-C. Chiang, *Phys. Rev. Lett.* **96**, 036802 (2006).
- <sup>10</sup>S.-J. Tang, L. Basile, T. Miller, and T.-C. Chiang, *Phys. Rev. Lett.* **93**, 216804 (2004).
- <sup>11</sup>G. Neuhold and K. Horn, *Phys. Rev. Lett.* **78**, 1327 (1997).
- <sup>12</sup>M. Miyazaki and H. Hirayama, *Surf. Sci.* **602**, 276 (2008).
- <sup>13</sup>K. Morgenstern, K.-F. Braun, and K.-H. Rieder, *Phys. Rev. Lett.* **89**, 226801 (2002).
- <sup>14</sup>K. Morgenstern, K.-H. Rieder, and G. A. Fiete, *Phys. Rev. B* **71**, 155413 (2005).
- <sup>15</sup>Y. Hasegawa and Ph. Avouris, *Phys. Rev. Lett.* **71**, 1071 (1993).
- <sup>16</sup>M. Watai and H. Hirayama, *Phys. Rev. B* **72**, 085435 (2005).
- <sup>17</sup>K. He, T. Hirahara, T. Okuda, S. Hasegawa, A. Kakizaki, and I. Matsuda, *Phys. Rev. Lett.* **101**, 107604 (2008).
- <sup>18</sup>L. Aballe, C. Rogero, P. Kratzer, S. Gokhale, and K. Horn, *Phys. Rev. Lett.* **87**, 156801 (2001).
- <sup>19</sup>I. Matsuda, T. Ohta, and H. W. Yeom, *Phys. Rev. B* **65**, 085327 (2002).
- <sup>20</sup>T.-C. Chiang, *Surf. Sci. Rep.* **39**, 181 (2000).
- <sup>21</sup>A. L. Wachs, A. P. Shapiro, T. C. Hsieh, and T.-C. Chiang, *Phys. Rev. B* **33**, 1460 (1986).
- <sup>22</sup>A. Zangwill, *Physics at Surfaces* (Cambridge University Press, Cambridge, 1988).
- <sup>23</sup>H. Ibach, *Surf. Sci. Rep.* **29**, 195 (1997).
- <sup>24</sup>P. Paniago, R. Matzdorf, G. Meister, and A. Goldmann, *Surf. Sci.* **336**, 113 (1995).